

Contribution from the Anorganisch-chemisches Institut, Universität Zürich, CH-8057 Zürich, Switzerland, and Institut für Anorganische Chemie, Universität Bern, CH-3000 Bern 9, Switzerland

The Creutz-Taube Complex Revisited: A Single-Crystal EPR Study

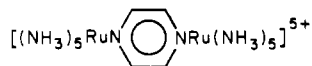
ANTON STEBLER,*^{1a} JOHN H. AMMETER,^{1a} URS FÜRHOLZ,^{1b} and ANDREAS LUDI^{1b}

Received September 30, 1983

Single-crystal EPR experiments have been performed on orthorhombic $[(\text{NH}_3)_5\text{Ru}(\text{pz})\text{Ru}(\text{NH}_3)_5]\text{Cl}_5 \cdot 5\text{H}_2\text{O}$ at 3 K. Two resonance lines appear in the crystallographic ab plane, one each from the two structurally equivalent binuclear ions with different orientation. The resonances are described by g tensors that have their principal axes collinear to the molecular axes. Both g_x components are parallel to the crystallographic c axis, which is perpendicular to the plane of the pyrazine rings. The angle between the Z axes (Ru-Ru line) of the two magnetically inequivalent complexes is $86(1)^\circ$ in agreement with X-ray diffraction results (85.5°). The components of the g tensor are $g_x = 1.346(3)$, $g_y = 2.799(3)$, and $g_z = 2.487(3)$. No Ru hyperfine structure could be observed owing to the large line width in the undiluted single crystal. The EPR spectrum was simulated by diagonalization of the 6×6 perturbation matrix using a one-center basis set in the hole formalism with the parameters $D/\lambda = 2.317(20)$, $E/\lambda = 0.745(20)$, and $K = 0.981(5)$. Both an axial and a rhombic component of the ligand field must be considered to reproduce the g tensor anisotropy. The orbital reduction factor k within the t_{2g}^5 configuration is estimated to be 0.79. The unpaired electron is predominantly in an orbital perpendicular to the plane of the pyrazine ring. Delocalization of the odd electron over the two ruthenium ions via the π^* system of the pyrazine ring is therefore possible.

Introduction

A series of experimental and theoretical studies have been devoted to the discussion of the electronic structure of the $(\mu\text{-pyrazine})\text{decaamminediruthenium(II,III)}$ ion



since its original preparation by Creutz and Taube.² Within the widely accepted classification scheme of Robin and Day,³ the central question deals with the extent of delocalization of the odd electron in this binuclear complex formally containing t_{2g}^6 Ru(II) and t_{2g}^5 Ru(III). The unique optical feature of the Creutz-Taube ion, a rather narrow intense ($\epsilon = 5500 \text{ M}^{-1} \text{ cm}^{-1}$) absorption band at low energy (6400 cm^{-1}) is attributed to the metal-metal interaction.

The results of the various experimental studies spanning a wide range of time scales, however, do not unambiguously resolve the issue "localized vs. delocalized". A comprehensive review of the pertinent literature and of the sometimes conflicting conclusions has been published recently by Creutz.⁴ This situation prompted us to start a reinvestigation of the Creutz-Taube complex exploiting the improvement in resolution of some physical techniques during the past decade. Moreover, some of the earlier experiments were hampered by small sample quantities, impurities, decomposed samples, and structural disorder. Special emphasis, therefore, was given to the preparation of pure and well-crystallized samples including the monovalent oxidized and reduced forms of the Creutz-Taube ion. A short publication summarized some important combined results from single-crystal X-ray studies, ⁹⁹Ru Mössbauer experiments, magnetic susceptibilities, electronic and vibrational spectroscopy, resonance Raman experiments, and an EPR study.⁵ A complete account of the EPR experiments on single crystals of $[(\text{NH}_3)_5\text{Ru}(\text{pz})\text{Ru}(\text{NH}_3)_5]\text{Cl}_5 \cdot 5\text{H}_2\text{O}$ (pz is pyrazine) is presented in this paper.

Experimental Section

Single crystals of $[(\text{NH}_3)_5\text{Ru}(\text{pz})\text{Ru}(\text{NH}_3)_5]\text{Cl}_5 \cdot 5\text{H}_2\text{O}$ were grown from aqueous solution either by the slow cooling of a saturated solution or by isothermal evaporation of the solvent. The specimens were dark purple needles, typically $1.5 \times 0.4 \times 0.4 \text{ mm}^3$ with the needle axis

parallel to the crystallographic c axis and showing well-developed $\{110\}$ faces. EPR measurements (X-band, Varian E-109) were performed with the magnetic field either in the YZ plane ($H \perp c$) or in the plane containing the c axis (X) and the normal to a (110) face. The microwave frequency was measured by using an EIP 350-D frequency counter and the magnetic field with a Varian NMR gaussmeter. The measurements were taken at 3 K by using an Oxford Instruments EPR-10 helium-flow cryostat with a VC 30 variable-temperature controller unit. The estimated accuracy of the temperature measured was $\pm 0.2 \text{ K}$. A goniometer was employed to rotate the single crystal inside the cavity about a vertical axis. The final crystal orientation in the cavity was found to be correct within $\pm 1^\circ$.

Theoretical Background

Crystal structure analysis shows the ruthenium atoms of the Creutz-Taube ion to be structurally equivalent for $[(\text{NH}_3)_5\text{Ru}(\text{pz})\text{Ru}(\text{NH}_3)_5]\text{Cl}_5 \cdot 5\text{H}_2\text{O}^6$ and $[(\text{NH}_3)_5\text{Ru}(\text{pz})\text{Ru}(\text{NH}_3)_5]\text{Br}_{10/3}\text{Cl}_{5/3} \cdot 4\text{H}_2\text{O}^7$ (Figure 1). Neglecting the protons the symmetry of the binuclear complex is $2/m$. The angle between the pyrazine plane and the $\text{cis-NH}_3\text{-Ru}$ bonds is 45° . The structure of each RuN_6 subunit may be described by an axial distortion along the $\text{trans-NH}_3\text{-Ru-N}(\text{pz})$ axis (Z , Figure 1). The orthogonal axes (x_a, y_a) in each subunit are passing through the centers of ligand atoms. Since this coordinate system is not symmetry adapted, we define new axes that also satisfy the EPR convention

$$E \leq \frac{2}{3}|D| \quad (1)$$

where D = tetragonal and E = rhombic components of the ligand field, respectively. The following definitions will be used:

sym-adapted single ion coord	single ion coord	mol coord of dimer
x	z_a	Z
y	$(1/2^{1/2})(x_a + y_a)$	X
z	$(1/2^{1/2})(y_a - x_a)$	Y

General theoretical expressions developed by Stevens,⁸ Kamimura,⁹ Bleaney and O'Brien,¹⁰ and Griffith¹¹ for the g tensor of a localized low-spin d^5 metal can be applied to the g values obtained for the Creutz-Taube ion. In low-spin d^5 complexes the unpaired electron occupies the t_{2g} orbitals, which

- (1) (a) Universität Zürich. (b) Universität Bern.
- (2) Creutz, C.; Taube, H. *J. Am. Chem. Soc.* **1969**, *91*, 3988; **1973**, *95*, 1086.
- (3) Robin, M. B.; Day, P. *Adv. Inorg. Chem. Radiochem.* **1967**, *10*, 247.
- (4) Creutz, C. *Prog. Inorg. Chem.* **1983**, *30*, 1.
- (5) Fürholz, U.; Bürgi, H. B.; Wagner, F. E.; Stebler, A.; Ammeter, J. H.; Krausz, E.; Clark, R. J. H.; Stead, M. J.; Ludi, A. *J. Am. Chem. Soc.* **1984**, *106*, 121.

- (6) Fürholz, U.; Ludi, A.; Bürgi, H. B., to be submitted for publication.
- (7) Beattie, J. K.; Hush, N. S.; Taylor, P. R.; Raston, C. R.; White, A. H. *J. Chem. Soc., Dalton Trans.* **1977**, 1121.
- (8) Stevens, K. W. H. *Proc. R. Soc. London, Ser. A* **1953**, *219*, 542.
- (9) Kamimura, H. *J. Phys. Soc. Jpn.* **1956**, *11*, 1171.
- (10) Bleaney, B.; O'Brien, M. *Proc. Phys. Soc., London, Sect. B* **1956**, *69*, 1216.
- (11) Griffith, J. S. "The Theory of Transition Metal Ions"; Cambridge University Press: New York, 1964.

Table I. Spin-Orbit Coupling, Low-Symmetry Ligand Field, and Zeeman Interaction Matrix for t_{2g} Levels^a

	$ xy^+\rangle$	$-(z^2 - y^2)^+$	$ xz^+\rangle$	$ xy^-\rangle$	$-(z^2 - y^2)^-$	$ xz^-\rangle$
$\langle xy^+ $	$\frac{2}{3}D + \beta H_z$	$-\lambda/2 - k\beta H_z i$	$-k\beta H_x i$	$g_e \beta H_- / 2$		$-\lambda/2$
$\langle -z^2 - y^2+ $	$\lambda/2 + k\beta H_z i$	$-D/3 + E/2 + \beta H_z$	$k\beta H_y i$		$g_e \beta H_- / 2$	$\lambda/2$
$\langle xz^+ $	$k\beta H_x i$	$-k\beta H_y i$	$-D/3 - E/2 + \beta H_z$	$\lambda/2$	$-\lambda/2$	$g_e \beta H_- / 2$
$\langle xy^- $	$g_e \beta H_x / 2$		$-\lambda/2$	$\frac{2}{3}D - \beta H_z$	$\lambda/2 - k\beta H_z i$	$-k\beta H_x i$
$\langle -z^2 - y^2- $		$g_e \beta H_x / 2$	$-\lambda/2$	$-\lambda/2 + k\beta H_z i$	$-D/3 + E/2 - \beta H_z$	$k\beta H_y i$
$\langle xz^- $	$\lambda/2$	$\lambda/2$	$g_e \beta H_x / 2$	$k\beta H_x i$	$-k\beta H_y i$	$-D/3 - E/2 - \beta H_z$

^a The Hamiltonian and the parameters D , E , and λ are defined in eq 4; $H_{\pm} = H_x \pm iH_y$.

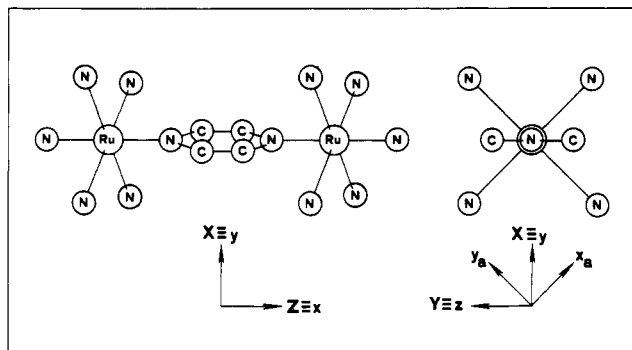


Figure 1. Molecular structure of $[(NH_3)_5Ru(pz)Ru(NH_3)_5]^{5+}$ and definition of the coordinate systems.

are split under the combined effect of noncubic ligand fields and spin-orbit coupling, which we assume to be isotropic. The problem is reduced to that of a single hole in the t_{2g} orbitals and is treated as the d^1 configuration with consequent change of sign for the spin-orbit coupling parameter λ and the low-symmetry field parameters D and E . For the first step, interaction between the ground state and excited configurations will be neglected since λ , D , and E are small compared to the excitation energy. However, they are taken into account later for the correction of the orbital reduction factor following the theory deduced by Hill.¹² Within this framework, the following t_{2g} one-electron orbitals are derived:

$$|xy\rangle = \frac{1}{2^{1/2}}\{|x_a z_a\rangle + |y_a z_a\rangle\} = \frac{1}{i2^{1/2}}\{|+2\rangle - |-2\rangle\} \quad (2a)$$

$$|xz\rangle = -\frac{1}{2^{1/2}}\{|x_a z_a\rangle - |y_a z_a\rangle\} = -\frac{1}{2^{1/2}}\{|+1\rangle - |-1\rangle\} \quad (2b)$$

$$|z^2 - y^2\rangle = -2|x_a y_a\rangle = \frac{3^{1/2}}{2}|0\rangle + \frac{1}{2(2^{1/2})}\{|+2\rangle + |-2\rangle\} \quad (2c)$$

where it can be shown that

$$|z^2 - y^2\rangle = \frac{3^{1/2}}{2}|z^2\rangle + \frac{1}{2}|x^2 - y^2\rangle \quad (3)$$

The Hamiltonian is written as

$$\hat{H} = \hat{H}_{\text{tet}} + \hat{H}_{\text{rhomb}} + \hat{H}_{\text{so}} + \hat{H}_{\text{Ze}} = \frac{D}{3}\left[\hat{L}_z^2 - \frac{1}{3}L(L+1)\right] + \frac{E}{12}(\hat{L}_+^2 + \hat{L}_-^2) + \lambda\hat{L}_z\hat{S}_z + \frac{\lambda}{2}(\hat{L}_+\hat{S}_- + \hat{L}_-\hat{S}_+) + \sum_{x,y,z}(K\hat{L}_i + g_e\hat{S}_i)\beta\hat{H}_i \quad (4)$$

The 6×6 matrix is given in Table I. The splitting of the one-electron levels for the t_{2g}^5 configuration in the presence of tetragonal and rhombic ligand field components and spin-orbit interaction is shown schematically in Figure 2. Neglecting the rhombic component of the ligand field, eigenvalues for the three Kramers doublets are obtained (Figure 3). Upon diagonalization of the 6×6 perturbation matrix, $|g_{\parallel}|$ and $|g_{\perp}|$

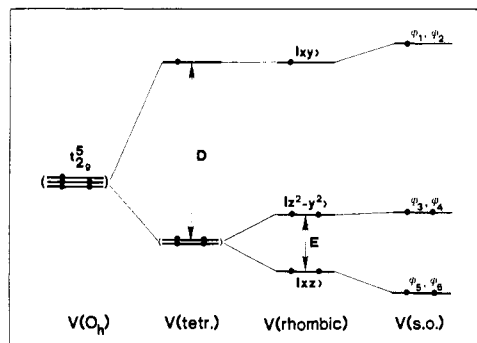


Figure 2. Schematic splitting of the one-electron levels for the t_{2g}^5 configuration under the influence of tetragonal and rhombic ligand field components and spin-orbit coupling. λ , D , and E are negative (cf. text).

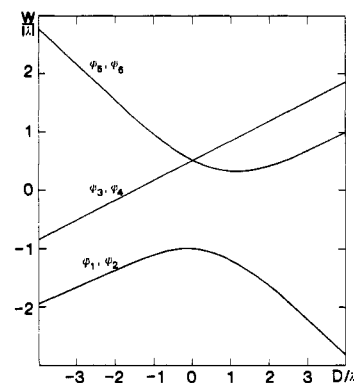


Figure 3. Splitting of the ${}^2T_{2g}$ energies of a low-spin d^5 ion under the effect of a tetragonal ligand field and spin-orbit coupling as a function of D/λ for $k = 1.0$.

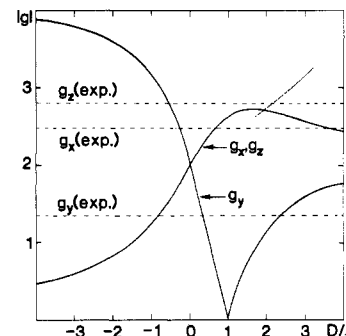


Figure 4. Values of the g components of a d^5 low-spin ion calculated as a function of the ratio D/λ for $k = 1.0$. The coordinate system is defined in Figure 1.

can be calculated as a function of the ratio D/λ (Figure 4).

The ground-state Kramers doublet can be written as

$$\Psi_1 = a|xy^+\rangle + b|(z^2 - y^2)^+\rangle + c|xz^-\rangle \quad (5a)$$

$$\Psi_2 = a|xy^-\rangle - b|(z^2 - y^2)^-\rangle + c|xz^+\rangle \quad (5b)$$

where the superscripts plus or minus indicate the spin state. $a^2 + b^2 + c^2 = 1$ is the normalization condition. Diagonali-

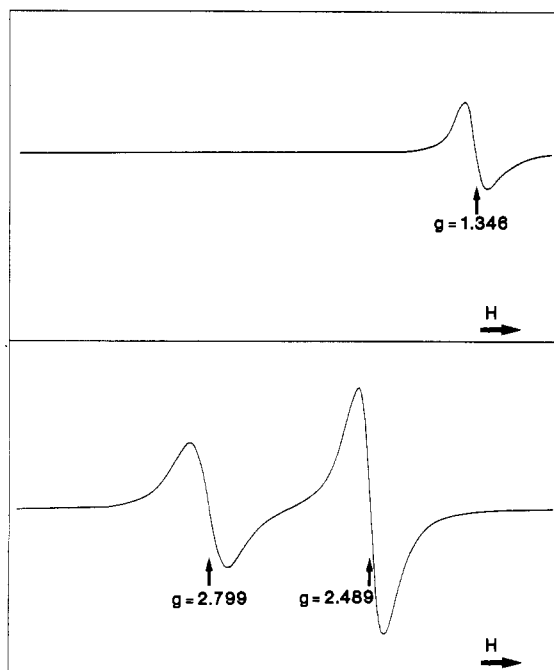


Figure 5. EPR spectra of a single crystal of $[(\text{NH}_3)_5\text{Ru}(\text{pz})\text{Ru}(\text{NH}_3)_5]\text{Cl}_5 \cdot 5\text{H}_2\text{O}$ at 3 K. The upper spectrum is taken with the magnetic field parallel to the crystallographic c axis and the lower one with the field in the ab plane along the Ru–Ru axis.

zation of the usual Zeeman perturbation within this ground-state doublet leads to the following components of the \mathbf{g} tensor:

$$\begin{aligned} |g_x| &= 2[a^2 - b^2 + c^2 - 2Kac] \\ |g_y| &= 2[a^2 - b^2 - c^2 + 2Kbc] \\ |g_z| &= 2[a^2 + b^2 - c^2 + 2Kab] \end{aligned} \quad (6)$$

K can be considered as an apparent orbital reduction factor of the t_{2g}^5 configuration including contributions from interactions with excited configurations, but it is not a measure of delocalization or covalency. Hill¹² has discussed the theory of the \mathbf{g} tensor for a low-spin d^5 ion considering effects of admixture of the excited $t_{2g}^4e_g$ configuration. The orbital reduction factor k in the t_{2g}^5 configuration can be related to K by

$$k = K / \{1 + (12B/E_{av})\} \quad (7)$$

where B is the Racah parameter and E_{av} an average excitation energy of the $t_{2g}^4e_g$ configuration. In addition it was shown that the spin–orbit coupling parameter λ should be replaced by

$$\Lambda = \lambda \{1 + (\lambda/E_{av})\} \quad (8)$$

Since λ for 4d ions is much smaller than E_{av} , this correction will be neglected in the following discussion.

Results

Figure 5 shows two EPR spectra of a single crystal of $[(\text{NH}_3)_5\text{Ru}(\text{pz})\text{Ru}(\text{NH}_3)_5]\text{Cl}_5 \cdot 5\text{H}_2\text{O}$ at 3 K, which agree with the experimental data reported earlier by Hush.¹³ The angular dependence of the g values of a single crystal rotated about the c axis is given in Figure 6. Two resonances appear in the ab plane since there are two crystallographically equivalent, but magnetically inequivalent, Creutz–Taube ions per unit cell (Figure 7). The resonances are described by two \mathbf{g} tensors that have their principal axes collinear to the molecular axes $X_A, Y_A,$ and Z_A of dimer A and $X_B, Y_B,$ and Z_B of dimer B, respectively. The g_x components of both magnetically in-

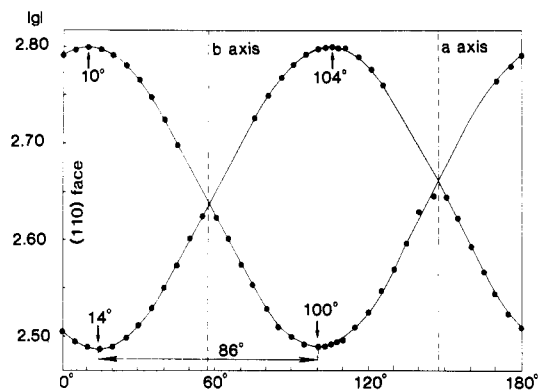


Figure 6. Angular dependence of the g values in the ab plane of a single crystal of $[(\text{NH}_3)_5\text{Ru}(\text{pz})\text{Ru}(\text{NH}_3)_5]\text{Cl}_5 \cdot 5\text{H}_2\text{O}$ at 3 K.

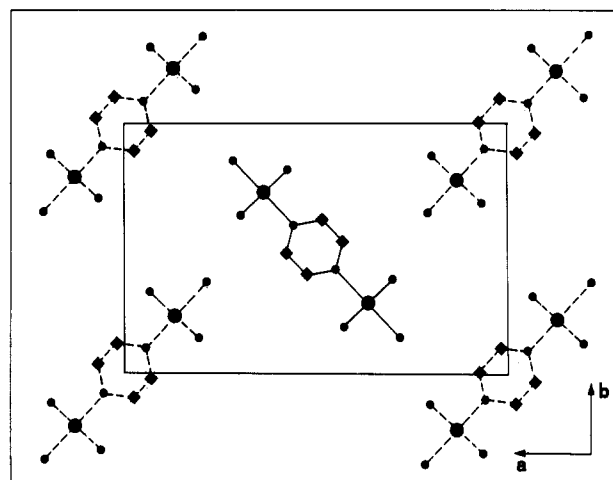


Figure 7. Projection of the unit cell of $[(\text{NH}_3)_5\text{Ru}(\text{pz})\text{Ru}(\text{NH}_3)_5]\text{Cl}_5 \cdot 5\text{H}_2\text{O}$ parallel to the crystallographic c axis (Cl atoms and H_2O are omitted): Ru, ●; N, •; C, ■.

equivalent dimers are parallel to the crystallographic c axis within the experimental error. Thus, the g_x axes are perpendicular to the plane of the pyrazine rings. The 86.1° angle between the g_{Z_A} and g_{Z_B} axes of the two structurally equivalent binuclear ions with different orientation is in agreement with diffraction results.^{6,7} Taking into account that the axes of the \mathbf{g} tensors are collinear to the molecular axes, the small deviation of this angle from 90° allows an unambiguous assignment of the EPR resonances to the molecular axes $X, Y,$ and Z . The g values and approximate line widths at 3 K are

$$g_x = g_y = 1.346 \quad (3) \quad \text{LW}_x = 170 \text{ G} \quad (9a)$$

$$g_Y = g_z = 2.799 \quad (3) \quad \text{LW}_Y \leq 70 \text{ G} \quad (9b)$$

$$g_Z = g_x = 2.487 \quad (3) \quad \text{LW}_Z \leq 50 \text{ G} \quad (9c)$$

The largest g value is in the plane of the pyrazine ring but perpendicular to the Ru–Ru axis. The line widths of the resonances gradually increase with temperature. At room temperature no EPR spectra of the Creutz–Taube complex could be observed. The average g value $([1/3(g_x^2 + g_y^2 + g_z^2)]^{1/2})$ of 2.30 (1) agrees well with the calculated mean g value obtained from susceptibility measurements ($g = 2.31$ (1)).¹⁴ No Ru hyperfine structure could be resolved even at 3 K due to the large line widths.

These results were checked with a single crystal of $[(\text{NH}_3)_5^{101}\text{Ru}(\text{pz})^{101}\text{Ru}(\text{NH}_3)_5]\text{Cl}_5 \cdot 5\text{H}_2\text{O}$. Within the experimental error no deviation from the results reported above could be observed. Although this single crystal was enriched

(13) Hush, N. S.; Edgar, A.; Beattie, J. K. *Chem. Phys. Lett.* **1980**, *69*, 128.

(14) Fürholz, U. Ph.D. Thesis, University of Bern, Bern, Switzerland, 1983.

with the ^{101}Ru isotope (93.1%) having a nuclear spin I of $5/2$, no hyperfine splitting was observed.

Discussion

The anisotropy of the g tensor of $[(\text{NH}_3)_5\text{Ru}(\text{pz})\text{Ru}(\text{NH}_3)_5]\text{Cl}_5 \cdot 5\text{H}_2\text{O}$ indicates that both an axial and a rhombic component of the ligand field have to be considered. This conclusion deviates from earlier assumptions.^{13,15} From a least-squares fit of the experimental g values to the analytical expressions of the g tensor components (eq 6) and considering the normalization condition, the coefficients of the lowest Kramers doublet a , b , c , and K are obtained:

$$\begin{aligned} a &= -0.9430 & b &= -0.2616 & c &= 0.2056 \\ & & K &= 0.981 \end{aligned} \quad (10)$$

Since these parameters are calculated only within the lowest Kramers doublet, the Zeeman interaction of the two excited Kramers doublets was taken into account by a subsequent diagonalization of the 6×6 matrix (Table I). The computation was performed in an iterative way with K fixed at 0.981. The EPR spectrum was simulated with the parameters

$$\begin{aligned} D/\lambda &= 2.317 \quad (20) & E/\lambda &= 0.745 \quad (20) \\ E/D &= 0.322 \end{aligned} \quad (11)$$

The following g values were obtained:

$$\begin{aligned} g_x &= g_y = 1.347 & g_y &= g_z = 2.800 \\ g_z &= g_x = 2.485 \end{aligned} \quad (12)$$

The wave functions of the lowest Kramers doublet are

$$\Psi_1 = -0.9430i|xy^+\rangle - 0.2618|(z^2 - y^2)^+\rangle + 0.2051|xz^-\rangle \quad (13a)$$

$$\Psi_2 = -0.9430i|xy^-\rangle + 0.2618|(z^2 - y^2)^-\rangle + 0.2051|xz^+\rangle \quad (13b)$$

The ratio E/D is about half of its maximum value, $E/|D| = 2/3$, where the three Kramers doublets would be equally spaced.

In order to calculate the absolute magnitudes of D and E , the spin-orbit coupling constant λ of the low-spin Ru^{3+} ion should be known. The free ion value has been reported to be $+1197 \text{ cm}^{-1}$.¹⁶ With an estimated value of -1000 cm^{-1} for this complex, the tetragonal component of the crystal field, D , is $-2317 \text{ (20) cm}^{-1}$ and the rhombic component, E , $-745 \text{ (20) cm}^{-1}$. These parameters yield the following eigenvalues for the three Kramers doublets:

$$\begin{aligned} E_1, E_2 &= -1793 \text{ (20) cm}^{-1} \\ E_3, E_4 &= 378 \text{ (20) cm}^{-1} & E_5, E_6 &= 1415 \text{ (20) cm}^{-1} \end{aligned} \quad (14)$$

Preliminary experiments show a broad band at about 2000 cm^{-1} in the infrared spectrum of the Creutz-Taube complex, compatible with the energy difference of the two lowest levels.

No such absorption can be detected for the oxidized and reduced monovalent species.¹⁷

The value of K indicates that some excited configuration contribution to the orbital angular momentum has to be taken into account as outlined above (eq 7). In this equation, E_{av} may be approximated by the ligand field parameter $10Dq$. With $30\,000 \text{ cm}^{-1}$ for $10Dq$ ^{18,19} and 600 cm^{-1} for the Racah parameter B , the orbital reduction factor k in the t_{2g}^5 configuration is obtained as

$$k = K/1.24 \approx 0.79 \quad (15)$$

This result shows that considerable spin density is shifted from metal orbitals into ligand orbitals. In addition, the reduction of k from the free ion value of 1.0 is of the same order as the reduction of λ from its free ion value in support of the previous estimate of λ .²⁰

The simulation of the experimental g tensor indicates that the tetragonal axis of the ligand field is in the plane of the pyrazine ring but perpendicular to the Ru-Ru line. This conclusion is in disagreement with results reported by Hush¹³ where rhombic distortions were neglected and the tetragonal axis was chosen normal to the pyrazine plane. The molecular geometry of the Creutz-Taube ion, as determined by single-crystal X-ray studies,^{6,7} however, shows the axial distortion to be parallel to the molecular Z axis. Clearly there is no apparent correlation of electronic properties as expressed by the g tensor to the overall molecular structure.

The wave functions of the ground-state Kramers doublet (eq 13) show that the unpaired electron is predominantly in the $|XZ\rangle$ orbital. This orbital is parallel to the π^* orbitals of the pyrazine ring as may be seen from Figure 1. Interaction between the two sets of orbitals and delocalization of the unpaired electron between the two Ru ions via the π^* system of the pyrazine ring is therefore possible.

Whereas the EPR results are thus compatible with a valence-delocalized ground state for the Creutz-Taube ion, it is not possible to estimate the extent of delocalization owing to the unresolved hyperfine structure. Also, a valence-trapped situation cannot be excluded from these experiments alone.

In conclusion, our EPR experiments demonstrate a considerable rhombic distortion in addition to the tetragonal component of the ligand field. In conjunction with structural data it can be unambiguously established that the unpaired electron of the Creutz-Taube ion is in an orbital suitable for metal-metal interaction. The experimentally determined orbital reduction factor moreover indicates a significant removal of spin density from the formally three-valent ruthenium ion.

Acknowledgment. This work was supported by the Swiss National Science Foundation under Grants 2.209-0.81 and 2.442-0.82.

Registry No. $[(\text{NH}_3)_5\text{Ru}(\text{pyz})\text{Ru}(\text{NH}_3)_5]\text{Cl}_5 \cdot 5\text{H}_2\text{O}$, 87922-20-1.

- (15) Bunker, B. C.; Drago, R. S.; Hendrickson, D. H.; Richman, R. M.; Kessel, S. T. L. *J. Am. Chem. Soc.* **1978**, *100*, 3805.
 (16) Blume, M.; Freeman, A. J.; Watson, R. E. *Phys. Rev. [Sect. A]* **1964**, *134*, 320.

- (17) Fürholz, U.; Bürgi, H. B.; Joss, S.; Ludi, A.; Krausz, E., to be submitted for publication.
 (18) Sakaki, S.; Hagiwara, N.; Yanase, Y.; Ohyashi, A. *J. Phys. Chem.* **1978**, *82*, 1971.
 (19) Stebler, A.; Bernhard, P.; Ludi, A. *Inorg. Chem.*, in press.
 (20) Abragam, A.; Bleaney, B. "Electron Paramagnetic Resonance of Transition Ions"; Clarendon Press: Oxford, 1970.